Noncanonical amino acid incorporation enables minimally disruptive labeling of stress granule and TDP-43 proteinopathy

Hao Chen[1, 2], Haocheng Wang[1], Yuning Lu[1, 2], Peng Chen[1, 2], Zhongfan Zheng[1, 2], Tao Zhang[1, 2], Jiou Wang[1, 2*]

[1] Department of Biochemistry and Molecular Biology, Bloomberg School of Public Health, Johns Hopkins University, Baltimore, MD, 21205, USA.

[2] Department of Neuroscience, School of Medicine, Johns Hopkins University, Baltimore, MD, 21205, USA.

*To whom correspondence should be addressed:

Jiou Wang, E-mail: jiouw@jhmi.edu

Key words: Genetic code expansion, Anap labeling, Stress granule, TDP-43

Abstract

We report a minimally disruptive labeling strategy for stress granule protein, G3BP Stress Granule Assembly Factor 1 (G3BP1), and ALS-linked protein, TAR DNA-binding protein 43 (TDP-43), using the fluorescent noncanonical amino acid Anap. By integrating genetic code expansion (GCE) with rational site selection, we achieved precise incorporation of Anap that preserves protein structure and function. In live cells and neurons, Anap labeling faithfully recapitulated localization, stress-induced dynamics, and recovery behavior, outperforming conventional fluorescent tags and enabling physiologically relevant visualization of protein pathobiology.

Introduction

Fluorescent protein labeling remains a cornerstone of live-cell biology, yet conventional techniques rely heavily on large fusion tags, such as auto-fluorescent tags (AFPs) or small-molecule-binding motifs[1], at limited positions (typically N-or C-terminal). These tags might potentially affect the structure, function, and even localization pattern of proteins, limiting their use for studying proteins with complex dynamics[2]. Alternatively, genetic code expansion (GCE) has emerged as a versatile labeling strategy to label proteins site-specifically in a minimally disruptive manner[3-8].

GCE employs an engineered orthogonal aminoacyl tRNA synthetase/tRNA pair to incorporate non-canonical amino acids (ncAAs) at desired positions of proteins according to reassigned codons, most commonly the amber stop codon (TAG), thereby introducing a single-residue substitution within the protein of interest. Among these ncAAs, L-Anap (3-(6-acetylnaphthalen-2-ylamino)-2-aminopropanoic acid) is especially attractive for live-cell imaging. Anap is intrinsically fluorescent, exhibits polarity-sensitive emission spectra, and requires no post-incorporation modification[2, 5]. Despite these advantages, GCE-based Anap labeling has rarely been systematically applied to track disease-relevant protein dynamics in live mammalian cells. In this study, we developed an Anap-based labeling platform optimized for minimally disruptive labeling of two important proteins, G3BP1 and TDP-43, involved in membraneless organelles and neurodegenerative diseases, such as amyotrophic lateral sclerosis (ALS) and frontotemporal dementia (FTD).

G3BP1 is a core protein in stress granules, dynamic membraneless organelles related to stress response[9]. Altered stress-granule dynamics have been associated with ALS/FTD[10, 11]; however, whether stress granules directly drive neurodegeneration remains debated, as several studies suggest that stress granules primarily function as protective stress responses[12]. TDP-43 cytoplasmic inclusion is a hallmark of ALS/FTD pathology[13] and is closely associated with

50 dysregulation of RNA metabolism, ultimately leading to cellular defects[14]. Conventional
51 fluorescent protein tags have enabled visualization of TDP-43 and G3BP1 in living cells;
52 however, these approaches can perturb the native biophysical properties of the proteins being
53 studied. For example, GFP or other fluorescently tagged TDP-43 usually requires additional
54 modifications, such as deletion of the nuclear localization signal (NLS)[15, 16], to induce
55 cytoplasmic inclusion formation. Such manipulations introduce non-physiological conditions that
56 may alter the native trafficking and aggregation behavior of TDP-43. As for G3BP1, tags like
57 GFP may also cause unexpected effects on the phase separation or other dynamics of the
58 protein. In contrast, Anap-based GCE strategy allows the minimally perturbative labeling and
59 visualization of protein localization and stress-induced redistribution while preserving native
60 protein architecture and function of both proteins. Importantly, the approach provides a
61 generalizable genetically encoded platform for quantitatively examining the behavior of ALS-
62 associated proteins in living cells. By enabling faithful monitoring of protein trafficking and
63 stress-granule dynamics without extensive protein engineering, Anap-based GCE can offer a
64 powerful strategy for probing molecular-scale mechanisms underlying ALS-linked
65 proteinopathies.

66

67 **Results and Discussion**

68 To implement the site-specific Anap incorporation system, we selected and generated two
69 amber mutants, G3BP1^{F337TAG} and TDP-43^{V100TAG}, using a combination of structural and
70 functional criteria: exclusion from functional domains or localization signals, absence of disease-
71 associated mutations, lack of post-translational modification, and low predicted structural impact
72 by AlphaFold models. For G3BP1, the selected site was chosen to minimize interference with
73 domains important for stress granule assembly, RNA binding, and protein-protein interactions.
74 For TDP-43, the incorporation site was selected to avoid the major functional domains involved

75 in RNA binding, nuclear localization, and aggregation-related behavior, thereby reducing the
76 likelihood that Anap incorporation would perturb its native trafficking or function. More generally,
77 we aimed to place the ncAA at positions likely to be solvent-accessible and tolerant of
78 substitution, while avoiding highly conserved or functionally essential residues. Incorporation of
79 Anap was achieved via co-expression of an orthogonal tRNA/synthetase pair in cells. To ensure
80 that the fluorescence signal observed in our experiments was specifically derived from site-
81 specific Anap incorporation rather than background fluorescence, we performed three control
82 conditions. Specifically, we tested: (1) cells cultured with the addition of Anap, (2) cells
83 expressing the Anap incorporation system with the addition of Anap, and (3) cells expressing
84 both the TAG-mutated protein plasmid and the Anap incorporation system but without the
85 addition of Anap. These control experiments were performed for both TDP-43 and G3BP1, and
86 no observable fluorescence signal was detected under any of these conditions (Supplementary
87 Fig. 1).

88 We first tested the feasibility of the Anap labeling system for G3BP1. In HeLa cells, G3BP1-
89 Anap localized diffusely in the cytoplasm under basal conditions, closely matching antibody
90 staining. Interestingly, a nuclear signal was detected with Anap but not with antibody, indicating
91 the presence of nuclear pools of G3BP1 inaccessible to antibody detection. Upon sodium
92 arsenite treatment, both the Anap and antibody signals colocalized within stress granules (Fig.
93 1A), validating the ability of Anap labeling to visualize the dynamics of G3BP1-driven stress
94 granule formation. In addition, to independently validate protein expression, we performed
95 western blot analysis in a G3BP knockout U2OS cell line, confirming the expression of G3BP1-
96 Anap (Fig. 1H). To assess labeling fidelity, we compared the performance of G3BP1-Anap with
97 G3BP1-GFP using fluorescence recovery after photobleaching (FRAP). Following stress, both
98 labeled proteins localized to granules, but G3BP1-Anap exhibited significantly higher
99 fluorescence recovery (~53%) than G3BP1-GFP (~33%) (Fig. 1C, 1F). These results suggest

100 that G3BP1-Anap displays higher mobility compared with G3BP1-GFP, indicating that Anap
101 labeling may provide a less perturbative approach for monitoring G3BP1 dynamics. Additionally,
102 we examined the colocalization of G3BP1-Anap with TIA-1, another established stress granule
103 marker. Under stress conditions, G3BP1-Anap largely colocalized with TIA-1 within stress
104 granules. Interestingly, under basal conditions, the nuclear signal of G3BP1-Anap, which was
105 not detected by antibody staining, appeared to partially colocalize with TIA-1 in several
106 condensate-like structures. (Fig. 1I).

107 We next applied Anap labeling to TDP-43. Under basal conditions, the signal of TDP-43-Anap
108 overlapped with that of anti-TDP-43 antibody staining, predominantly within the nucleus (Fig.
109 1B). Following sodium arsenite treatment, TDP-43-Anap mislocalized mostly to the cytoplasmic
110 inclusions stained by TDP-43 antibody, with noticeable difference that a few puncta showed
111 Anap signal only, and antibody gave more dispersed signal. By contrast, TDP-43-YFP failed to
112 recapitulate this cytoplasmic mislocalization, instead forming prominent nuclear puncta under
113 stress conditions (Fig. 1E), suggesting that large C-terminal tags may distort native localization
114 of the protein. We then used YFP-tagged NLS-deleted TDP-43 (TDP-43$^{\Delta NLS}$-YFP) as a
115 reference and performed FRAP analysis to compare the mobility of TDP-43-Anap and TDP-
116 43$^{\Delta NLS}$-YFP. Fluorescence recovery of TDP-43-Anap reached ~45% within 20 s after
117 photobleaching, consistent with liquid-like dynamics. In contrast, TDP-43$^{\Delta NLS}$-YFP showed only
118 ~22% recovery, suggesting more solid-like dynamics (Fig. 1D, 1G). These results are consistent
119 with previous reports describing relatively immobile aggregates formed by TDP-43$^{\Delta NLS}$[16]and
120 illustrate the advantage of Anap-based labeling, which preserves native protein properties and
121 enables real-time assessment of protein dynamics without introducing disruptive mutations. To
122 further investigate the relationship between TDP-43-Anap-positive cytoplasmic inclusions and
123 stress granules, we performed co-immunostaining with a G3BP1 antibody. Under stress
124 conditions, most TDP-43-Anap-positive cytoplasmic inclusions colocalized with G3BP1-positive

125 stress granules. However, a small subset of puncta contained TDP-43-Anap but lacked
126 detectable G3BP1, suggesting that not all mislocalized TDP-43 is incorporated into stress
127 granules under oxidative stress. These observations raise the possibility that additional
128 mechanisms may contribute to the formation of TDP-43-positive cytoplasmic puncta (Fig. 1J).

129 To determine whether TDP-43-Anap retains biological function, we expressed it in a TDP-43
130 knockout HeLa cell line (Fig. 1K) and tested cell viability under oxidative stress. Following 12.5
131 μM sodium arsenite treatment for 24 hours, the expression of TDP-43-Anap significantly
132 rescued cell survival, reaching levels comparable to wild-type TDP-43 overexpression (45% vs
133 46%; Fig. 1M). We further validated this finding in a mouse embryonic stem (ES) cell model with
134 an inducible TDP-43 knockout (iTDPKO). For mouse ES cells, TDP-43 KO alone was sufficient
135 to induce cell death. Here, either wild-type TDP-43 or TDP-43-Anap was expressed in iTDPKO
136 mouse ES cells, where TDP-43 was deleted following induction with 4-hydroxytamoxifen (4-HT).
137 Expression of TDP-43-Anap restored ES cell viability nearly to wild-type TDP-43 (47% vs 51%;
138 Fig. 1N). We also evaluated TDP-43-dependent RNA splicing activity by examining the
139 expression of PFKP, a well-established target that undergoes cryptic exon inclusion upon loss of
140 TDP-43 function[17]. As shown in Figures 1K and 1L, expression of TDP-43-Anap in TDP-43
141 knockout HeLa cells restored PFKP expression, indicating that the Anap-labeled protein retains
142 functional RNA splicing activity. These results demonstrate that TDP-43-Anap is capable of
143 functionally compensating for endogenous TDP-43, supporting that the incorporation of Anap
144 does not substantially disrupt the protein's biological function.

145 Furthermore, to extend Anap labeling to neuronal systems, we applied this approach to label
146 both proteins in primary mouse cortical neurons. The neurons were co-stained with human-
147 specific anti-TDP-43 or human-specific anti-G3BP1 antibodies. Under basal conditions, the
148 signal of G3BP1-Anap colocalized with antibody staining in the cytoplasm and relocalized to
149 stress granule upon sodium arsenite treatment (Fig. 2A, 2B). Notably, nuclear Anap signal was

150 again observed in neurons, suggesting additional pools of G3BP1 not captured by antibody
151 staining.

152 TDP-43-Anap localized to the neuronal nucleus under basal conditions and showed strong
153 colocalization with anti-TDP-43 antibody. Interestingly, antibody staining appeared more
154 diffusely cytoplasmic than Anap, suggesting improved signal specificity of Anap labeling with
155 direct genetic incorporation. Under oxidative stress, both Anap and antibody signals colocalized
156 within cytoplasmic inclusions (Fig. 2C, 2D). These findings demonstrated that the Anap system
157 for G3BP1 and TDP-43 performs robustly in neuronal environments, a key setting for ALS/FTD
158 research.

159 In summary, our results demonstrated that Anap-based GCE provides a minimally disruptive
160 strategy for tracking the dynamic behavior of G3BP1 and TDP-43 in live cells (Fig. 3). In
161 G3BP1, Anap faithfully reported stress granule assembly and preserved native mobility, unlike
162 GFP fusions that impaired dynamics. In TDP-43, Anap labeling maintained nuclear localization
163 under basal conditions and revealed liquid-like behavior of cytoplasmic inclusions during stress,
164 in contrast to the aberrant nuclear puncta produced by YFP-tagged TDP-43. Critically, Anap-
165 labeled TDP-43 retained biological activity, rescuing cell survival in TDP-43-deficient HeLa and
166 stem cells. Moreover, we have generated stable TDP-43-Anap cell lines that exhibited
167 consistent expression, protein localization, and stress-induced aggregation, providing stable cell
168 models for TDP-43 research.

169 By enabling high-fidelity visualization of both stress granule dynamics and TDP-43 aggregation
170 in live cells and primary neurons, Anap labeling bridges a critical gap between structural
171 preservation and functional readout. The ability to monitor native protein behavior without
172 perturbation provides a unique opportunity to study early events in ALS/FTD progression, such
173 as stress granule maturation, protein cytoplasmic mislocalization, and aggregate fluidity, at a
174 resolution inaccessible with conventional tagging approaches.

175 **Acknowledgements**

176 This work was supported by the National Institute of Health (NIH) (NS074324, NS089616,
177 NS110098, and NS128494) and the Walder Foundation. We thank Peter G. Schultz from
178 Scripps Research for providing the pAnap plasmid, Shawn M. Ferguson from Yale University for
179 the TDP-43 knockout HeLa cell line, J. Paul Taylor from St. Jude Children's Research Hospital
180 for the G3BP knockout U2OS cell line, and Philip Wong from Johns Hopkins University for the
181 iTDPKO mouse ES cell line. We also thank the members of Wang's lab for discussion and
182 suggestions.

183 **Author contributions**

184 H.C. performed and analyzed most of the experiments. H.C.W. helped with plasmid preparation,
185 western blot, and imaging. Y.N.L. provides cells and helped with data preparation. P.C. provides
186 mouse primary cortical neurons. Z.F.Z helped with imaging. T.Z. helped culture iTDPKO mouse
187 ES cells. H.C. and J.W. designed the studies and wrote the paper with inputs from other
188 authors.

189 **Methods and materials**

190 **General information**

191 Oligonucleotide synthesis was performed by IDT, and Sanger sequencing of DNA plasmids and
192 PCR products was performed by Quintara. L-ANAP (trifluoroacetate salt) (15436) used in this
193 study was purchased from Cayman. For immunostaining, the following primary and secondary
194 antibodies were used: mouse anti-human G3BP (BD Biosciences, 611126), rabbit anti-TDP-43
195 (Proteintech, 10782-2-AP), mouse anti-TDP-43 (human-specific, monoclonal; Proteintech,
196 60019-2-Ig), Rabbit anti-human TIA-1 (MBL Life science, RN014P), chicken anti-βIII-tubulin
197 (Tuj1; GeneTex, GTX85469), donkey anti-mouse Alexa Fluor 555 (Thermo Fisher, A-31570),
198 donkey anti-rabbit Alexa Fluor 488 (Thermo Fisher, A-21202), donkey anti-chicken Alexa Fluor

199 647 (Thermo Fisher, A78952), and donkey anti-rabbit Alexa Fluor Plus 800 (Thermo Fisher,
200 A32808).

201 **Plasmids**

202 pAnap plasmid was a gift from Peter G. Schultz's lab[2]. pCMV-G3BP1 was purchased from Sino
203 Biologics. pRK5-TDP-43, pEGFP-G3BP1, and pCMV/TO-TDP-43-YFP were conducted by our
204 lab. pLVX-Puro-TDP-43-WT was a gift from Shawn Ferguson's lab[18] and reconstructed into
205 pLVX-Puro-TDP-43-ΔNLS. Site-directed mutagenesis was conducted using the NEB Q5 site-
206 directed mutagenesis kit (NEB, E0554). TAG substitutions were introduced by PCR amplification
207 with Q5 Hot Start High-Fidelity DNA Polymerase using primers designed with NEBaseChanger.
208 Then the PCR products were incubated with an enzyme mix consisting of a kinase, a ligase,
209 and DpnI to rapidly circularize the PCR products and remove the template DNA. And then the
210 mix will be transformed into DH5α cells.

211 **Cell culture**

212 Mammalian cell lines were cultured at 37°C and 5% CO_2 in humidified incubators. HeLa cells
213 (ATCC) were cultured in DMEM/F12 (Corning, 10-013-CV) supplemented with 10% FBS (Gibco,
214 A5256801). The TDP-43 knockout HeLa cell line was a gift from Shawn M. Ferguson[18] and the
215 G3BP knockout U2OS cell line was a gift from J. Paul Taylor[9]. Primary cortical neurons were
216 prepared as previously described [19]. Briefly, the cortex of the mouse embryo was separated into
217 HBSS on ice, then digested into single-cell suspension with 0.25% trypsin and 0.1mg/ml DNase
218 I at 37°C for 20 min. Dissociated cells were washed twice and resuspended in plating media
219 (DMEM supplemented with 10% FBS) before seeding onto poly-D-lysine (Gibco, A3890401)-
220 coated plates. Cells were cultured for 3-4 hours in plating medium to settle down, and then the
221 medium was replaced with maintenance medium (neurobasal medium (Gibco, 21103049))
222 supplemented with 2% B-27 supplement (Gibco,17504044), 1% GlutaMax (Gibco, 35050061),
223 and 1% penicillin/streptomycin (Gibco, 15140163). The iTDPKO inducible mouse embryonic

224 stem ES cell line was a gift from Philip Wong[20]. Cells were maintained on attachment factor
225 (Gibco, S-006-100) coated plates in 2i media containing half of DMEM/F12 and half of
226 Neurobasal media complemented with L-Glutamine (Gibco, 25030081), B-27 supplement, N2
227 supplement (Gibco, 17502048), BSA (Gibco, 15260037), 1% penicillin/streptomycin (Gibco,
228 15140163), PD0325901 (MedChemExpress, 391210-10-9), CHIR99021(MedChemExpress,
229 252917-06-9), monothioglycerol(Millipore Sigmal, M6145), and mLIF(Millipore Sigma,
230 ESG1107).

231 **Transfection**

232 HeLa cells were transfected using Lipofectamine 2000 reagent (ThermoFisher, 11668030). Cells
233 were seeded 24 h before transfection, and plasmid DNA was mixed with Lipofectamine 2000 at
234 a ratio of 1 μg DNA:2 μL reagent in Opti-MEM medium (Thermo Fisher, 31985070). After 15 min
235 incubation at room temperature, the complexes were added to the cells. Six hours post-
236 transfection, the medium was replaced with fresh growth medium supplemented with or without
237 20 μM L-Anap, and cells were incubated overnight before further experiments.

238 Mouse primary cortical neurons and inducible TDP-43 knockout (iTDPKO) mouse ES cells were
239 transfected using Lipofectamine 3000 (Thermo Fisher, L3000015) according to the
240 manufacturer's instructions. For neurons, first, the total DNA was diluted and mixed with p3000
241 reagent in Opti-MEM media, and the Lipofectamine 3000 was diluted in Opti-MEM media
242 separately. Second, both diluted DNA and Lipofectamine 3000 were mixed and incubated at
243 room temperature for 15 minutes. The final mix would then be added to cells seeded on poly-D-
244 lysine-coated plates at DIV5. After incubation overnight, the media were half-replaced with fresh
245 neurobasal media with 10μM Anap, and the neurons were incubated for two additional days (the
246 media were half-replaced each day to keep the Anap supply). Differently, for mouse ES cells,
247 the DNA-lipo3000 mix was added directly into the cell suspension, and the suspension was

248 added to attachment factor-coated plate. After overnight incubation, the media for ES cells was
249 replaced with fresh 2i media supplemented with 10 μM Anap and any further treatments.

250 **Anap labeling and immunofluorescence in cell fixation**

251 6h post-transfection, the cells were cultured in medium supplemented with L-Anap for another
252 20-24 h. Cells were then washed three times with DPBS to remove excess Anap and incubated
253 in fresh medium for 1 h before treatment with 250 μM sodium arsenite for anther 1h. After the
254 treatment, the cells were washed with DPBS three times and then fixed with 4%
255 paraformaldehyde (PFA; Millipore Sigma, 158127) for 15-20 mins at room temperature. Fixed
256 cells were permeabilized and blocked in immunofluorescence blocking buffer (Cell Signaling
257 Technology, 12411) containing 0.1% Triton X-100 (Millipore Sigma, X100) for 45 mins.
258 Immunostaining was performed using anti-TDP-43 and anti-G3BP1 antibodies in both HeLa
259 cells and primary cortical neurons, with anti-Tuj1 antibody included as a neuronal marker.
260 Images were acquired using a Leica SP8 confocal microscope.

261 **Anap labeling and GFP/YFP tagging in live-cell imaging**

262 For Anap labeling, HeLa cells were seeded on 35-mm glass-bottom dishes (Cellvis, D35-20-
263 1.5H), transfected, and incubated with L-Anap following the same protocol used for fixed-cell
264 imaging. After removal of excess Anap, cells were cultured in fresh medium for 2-3 h before live
265 cell imaging. For GFP/YFP tagging, cells expressing the tagged proteins were directly ready for
266 live cell imaging. Before FRAP, cells expressing Anap-labeled or GFP/YFP-tagged TDP-43 or
267 G3BP1 were treated with 250 μM sodium arsenite for 1 h. Next, regions of interest (ROIs)
268 corresponding to protein signals were selected for FRAP analysis using a Leica SP8 confocal
269 microscope.

270 **Cell survival tests**

271 Cell viability was assessed using Calcein AM staining (Invitrogen, C1430). HeLa cells were
272 treated with 12.5 μM sodium arsenite for 24 h, followed by incubation with 3 μM Calcein AM.

273 Fluorescence from viable cells was measured using a Synergy H1 Hybrid Multi-Mode Plate
274 Reader (BioTek) at excitation/emission wavelengths of 485/535 nm.

275 For mouse ES cells, the conditional knockout of TDP-43 was induced by 4-hydroxytamoxifen (4-
276 HT, Millipore Sigma, H7904-5MG) treatment (300ng/ml) for 5 days. Cell viability was assessed
277 using the Cell Counting-Lite 2.0 Luminescent Cell Viability Assay Kit (Vazyme, DD1101-02).

278 **Immunoblotting**

279 Cells were washed three times with PBS and lysed in ice-cold RIPA buffer [50 mM Tris-HCl (PH
280 7.5), 150 mM NaCl, 1% NP40, 0.1% SDS, 100 mM NaF, 0.5% sodium deoxycholate, 17.5 mM
281 beta-glycerophosphate, 1 mM PMSF, and protease inhibitor cocktail (1:200, Millipore Sigma,
282 P8340)]. Lysates were sonicated and clarified by centrifugation (12,000 rpm, 20 min, 4 °C), and
283 supernatants were collected. Protein concentrations were determined using the BCA assay
284 (Thermo Fisher, Cat. No. 23225). Equal amounts of protein were resolved by SDS-PAGE and
285 transferred to membranes, which were blocked with 5% BSA and incubated with primary
286 antibodies overnight at 4 °C. After three washes with TBST, membranes were incubated with
287 fluorescence-conjugated secondary antibody dilution at room temperature for 2h. Blots were
288 scanned and imaged by LI-COR Odyssey M scanner.

289 **Image analysis and statistical analysis**

290 All images were processed and analyzed by Fiji/ImageJ software, and the colocalization of
291 signals was analyzed by the colocalization threshold analysis plugin in ImageJ. Experiments
292 requiring quantification were repeated at least three times independently. The FRAP results
293 were analyzed by ImageJ to quantify the fluorescence intensity at each time point. The average
294 relative intensities (normalized to pre-bleaching intensity) of each time point were analyzed in
295 Prism 10 software. For survival tests, the average relative rates (normalized to the control
296 group) for each group were analyzed in Prism 10 software, and the one-way analysis of

297 variance (ANOVA) was used to compare the significance between each group. All data were

298 presented as means ± SEM.

References:

1. Crivat, G. & Taraska, J.W. Imaging proteins inside cells with fluorescent tags. *Trends in biotechnology* **30**, 8–16 (2012).
2. Chatterjee, A., Guo, J., Lee, H.S. & Schultz, P.G. A Genetically Encoded Fluorescent Probe in Mammalian Cells. *Journal of the American Chemical Society* **135**, 12540–12543 (2013).
3. Hao, M. et al. Tracking endogenous proteins based on RNA editing-mediated genetic code expansion. *Nat Chem Biol* **20**, 721–731 (2024).
4. Nikić, I., Kang, J.H., Girona, G.E., Aramburu, I.V. & Lemke, E.A. Labeling proteins on live mammalian cells using click chemistry. *Nature Protocols* **10**, 780–791 (2015).
5. Nygaard, A., Zachariassen, L.G., Larsen, K.S., Kristensen, A.S. & Loland, C.J. Fluorescent non-canonical amino acid provides insight into the human serotonin transporter. *Nature Communications* **15**, 9267 (2024).
6. Bessa-Neto, D. et al. Bioorthogonal labeling of transmembrane proteins with non-canonical amino acids unveils masked epitopes in live neurons. *Nature Communications* **12**, 6715 (2021).
7. Eddins, A.J. et al. Quantitative Protein Labeling in Live Cells by Controlling the Redox State of Encoded Tetrazines. *Journal of the American Chemical Society* **147**, 23625–23634 (2025).
8. Arsić, A., Hagemann, C., Stajković, N., Schubert, T. & Nikić-Spiegel, I. Minimal genetically encoded tags for fluorescent protein labeling in living neurons. *Nature Communications* **13**, 314 (2022).
9. Yang, P. et al. G3BP1 is a tunable switch that triggers phase separation to assemble stress granules. *Cell* **181**, 325–345 (2020).
10. Kassouf, T. et al. Targeting the NEDP1 enzyme to ameliorate ALS phenotypes through stress granule disassembly. *Science Advances* **9**, eabq7585 (2023).
11. Van Nerom, M. et al. C9orf72-linked arginine-rich dipeptide repeats aggravate pathological phase separation of G3BP1. *Proceedings of the National Academy of Sciences* **121**, e2402847121 (2024).
12. Wolozin, B. & Ivanov, P. Stress granules and neurodegeneration. *Nat Rev Neurosci* **20**, 649–666 (2019).
13. Neumann, M. et al. Ubiquitinated TDP-43 in Frontotemporal Lobar Degeneration and Amyotrophic Lateral Sclerosis. *Science* **314**, 130–133 (2006).
14. Suk, T.R. & Rousseaux, M.W.C. The role of TDP-43 mislocalization in amyotrophic lateral sclerosis. *Molecular Neurodegeneration* **15**, 45 (2020).
15. Gasset-Rosa, F. et al. Cytoplasmic TDP-43 De-mixing Independent of Stress Granules Drives Inhibition of Nuclear Import, Loss of Nuclear TDP-43, and Cell Death. *Neuron* **102**, 339–357.e337 (2019).
16. Yan, X. et al. Intra-condensate demixing of TDP-43 inside stress granules generates pathological aggregates. *Cell* **188**, 4123–4140.e4118 (2025).
17. Rothstein, J.D. et al. Sporadic ALS induced pluripotent stem cell derived neurons reveal hallmarks of TDP-43 loss of function. *Nature Communications* **16**, 7092 (2025).
18. Roczniak-Ferguson, A. & Ferguson, S.M. Pleiotropic requirements for human TDP-43 in the regulation of cell and organelle homeostasis. *Life Sci Alliance* **2** (2019).
19. Chen, P. et al. Spine impairment in mice high-expressing neuregulin 1 due to LIMK1 activation. *Cell Death & Disease* **12**, 403 (2021).
20. Chiang, P.-M. et al. Deletion of TDP-43 down-regulates Tbc1d1, a gene linked to obesity, and alters body fat metabolism. *Proceedings of the National Academy of Sciences* **107**, 16320–16324 (2010).

348 **Figure legend**

349 **Fig. 1: Anap-based labeling enables visualization of TDP-43 and G3BP1.**

350 A, B. HeLa cells expressing G3BP1-Anap and TDP-43-Anap under basal conditions or 250 μM
351 sodium arsenite treatment. Anap and antibody signals are shown in blue and green,
352 respectively; for merged channels, Anap was pseudo-colored red. Scale bars: 10 μm (overview),
353 3 μm (zoom). C, D. FRAP of G3BP1-Anap, G3BP1-GFP, and TDP-43-Anap, following 250 μM
354 sodium arsenite treatment. One granule from each of three independent cells was selected and
355 photobleached for FRAP analysis. ROI signal intensities are displayed in rainbow RGB (red-
356 high, blue-low). Scale bars: 5 μm (cells), 1 μm (ROI). E. Comparison of HeLa cells expressing
357 TDP-43-Anap and TDP-43-YFP under basal conditions or 250 μM sodium arsenite treatment.
358 Here, Anap labeling and YFP labeling yield a blue signal and a yellow to green signal,
359 respectively. F, G. Relative fluorescence recovery of each time point after photobleaching for
360 G3BP1-Anap, G3BP1-GFP, TDP-43-Anap and TDP-43$^{\Delta NLS}$-YFP. Here, error bars with filled area
361 are used for data presentation. FRAP recovery curves were compared using two-way ANOVA.
362 H. Immunoblotting of wild-type and Anap labeled G3BP1. The mouse anti-G3BP1 antibody was
363 used. KO: G3BP knock out; F337Stop/Anap: the expression of G3BP1^{F337TAG} via Anap labeling
364 without or with the addition of Anap. I. Colocalization of G3BP1-Anap with TIA-1. The mouse
365 anti-G3BP1 antibody and rabbit anti-TIA-1 antibody were used. Anap, G3BP1-Ab, and TIA-1-Ab
366 signals are shown in blue, grey and green, respectively; for merged channels, Anap was
367 pseudo-colored red. Scale bars: 10 μm (overview), 3 μm (zoom). J. Colocalization of TDP-43-
368 Anap with G3BP1. The mouse anti-G3BP1 antibody and rabbit anti-TDP-43 antibody were
369 used. Anap, TDP-43-Ab, and G3BP1-Ab signals are shown in blue, grey, and green,
370 respectively; for merged channels, Anap was pseudo-colored red. Scale bars: 10 μm (overview),
371 3 μm (zoom). K. Immunoblotting of wild-type TDP-43, TDP-43-Anap and PFKP proteins in TDP-
372 43 knockout HeLa cells. The Rabbit anti-TDP-43 antibody and rabbit anti-PFKP antibody were

373 used. KO: TDP-43 knockout; V100Stop/Anap: the expression of TDP-43^{V100TAG} via Anap labeling
374 without or with the addition of Anap. L. The expression levels of PFKP in TDP-43 knockout HeLa
375 cells expressing wide-type TDP-43 or TDP-43-Anap. One-way ANOVA was used to compare the
376 levels among groups. M. Survival of TDP-43 knockout HeLa cells expressing TDP-43-Anap after
377 treatment with 12.5 μM sodium arsenite for 24h. Calcien EM staining was used to quantify cell
378 survival, and the relative survival rate was calculated as the ratio of sodium arsenite-treated to
379 untreated cells for each group. OE: overexpression of TDP-43. One-way ANOVA was used to
380 compare levels among groups. N. Survival of iTDPKO inducible mouse ES cells expressing
381 TDP-43-Anap. Here, cell counting-Lite 2.0 Luminescent cell viability assay kit was used to
382 detect the survival rate of ES cells. TDP-43 knockout was induced by 4-HT (300ng/ml) for 5
383 days. The relative survival rate= 4-HT induction/DMSO for each group. One-way ANOVA was
384 used to compare levels among groups. Colocalization threshold analysis was performed in
385 Fiji/ImageJ to calculate the Pearson correlation coefficient (R) for each region of interest (A, B, I,
386 J). The X and Y axes represent the fluorescence intensity values of the red and green channels,
387 respectively. When signals are colocalized, pixels with high intensity in one channel correspond
388 to high intensity in the other, forming a diagonal distribution. In contrast, non-colocalized signals
389 cluster along the axes. A higher R value indicates a greater degree of colocalization. Scale bar,
390 3 μm. All quantitative data (F, G, L, M, N) are shown as mean ± SEM. ***P = 0.0001; ****P <
391 0.0001; n.s., not significant.

392 **Fig. 2: Anap labeling of TDP-43 and G3BP1 in neurons.**

393 A, C. Primary mouse cortical neurons expressing G3BP1-Anap and TDP-43-Anap under basal
394 conditions or 250 μM sodium arsenite treatment. Cells were stained with anti-G3BP1 (human-
395 specific) or anti-TDP-43 (human-specific) antibodies with chicken anti-Tuj1 as a neuron marker.
396 Signals: Anap (blue, pseudo-colored red in merged images), antibody (green), Tuj1 (gray).
397 Scale bar, 10 μm. B, D. The colocalization level of each region of interest for G3BP1 and TDP-
398 43. Colocalization threshold analysis was performed in Fiji/ImageJ to calculate the Pearson
399 correlation coefficient (R) for each region of interest. The X and Y axes represent the
400 fluorescence intensity values of the red and green channels, respectively. When signals are
401 colocalized, pixels with high intensity in one channel correspond to high intensity in the other,
402 forming a diagonal distribution. In contrast, non-colocalized signals cluster along the axes. A
403 higher R value indicates a greater degree of colocalization. Scale bar, 1 μm.

404 **Fig. 3: Schematic of the Anap labeling system for G3BP1 and TDP-43 using genetic code**
405 **expansion.**

406 Briefly, two plasmids were required to express the protein with site-specific Anap incorporation,
407 one for Anap incorporation and one for the mutated protein of interest (TAG introduction). As the
408 plasmids were transfected into cells, the orthogonal Anap-tRNA synthetase would charge the
409 Anap, a fluorescent amino acid, to its cognate tRNA, and the tRNA would incorporate the Anap
410 site-specifically into the protein of interest in response to the TAG stop codon. Cells expressing
411 Anap-labeled TDP-43 and G3BP1 were subsequently imaged by confocal microscopy, either
412 after fixation or in live-cell conditions. Upon stress conditions, TDP-43-Anap redistributes to the
413 cytoplasmic inclusions, and G3BP1-Anap assembles into stress granule.

414

415 **Supplementary Fig. 1: Controls for Anap-based labeling of TDP-43 and G3BP1 in HeLa**
416 **cells**

417 A. Controls for TDP-43-Anap labeling. Four experimental conditions were tested: (1) HeLa cells
418 expressing both the TAG-mutated TDP-43 plasmid and the Anap incorporation system in the
419 presence of Anap (TDP-43-Anap); (2) cells expressing both plasmids without Anap (TDP-43-
420 Stop); (3) cells cultured with Anap only; and (4) cells expressing the Anap incorporation system
421 with the addition of Anap. Signals for TDP-43-Anap, TDP-43 antibody staining, and G3BP1
422 antibody staining are shown in blue, grey, and green, respectively. The Anap signal is pseudo-
423 colored red in the merged images. B. Controls for G3BP1-Anap labeling. The same four
424 conditions were tested: (1) cells expressing the TAG-mutated G3BP1 plasmid and the Anap
425 incorporation system in the presence of Anap (G3BP1-Anap); (2) cells expressing both plasmids
426 without Anap (G3BP1-Stop); (3) cells cultured with Anap only (+ Anap only); and (4) cells
427 expressing the Anap incorporation system with the addition of Anap (Anap system+Anap).
428 Signals for G3BP1-Anap, G3BP1 antibody staining, and TIA-1 antibody staining are shown in
429 blue, grey, and green, respectively. The Anap signal is pseudo-colored red in the merged
430 images. Scale bars, 40 μm.

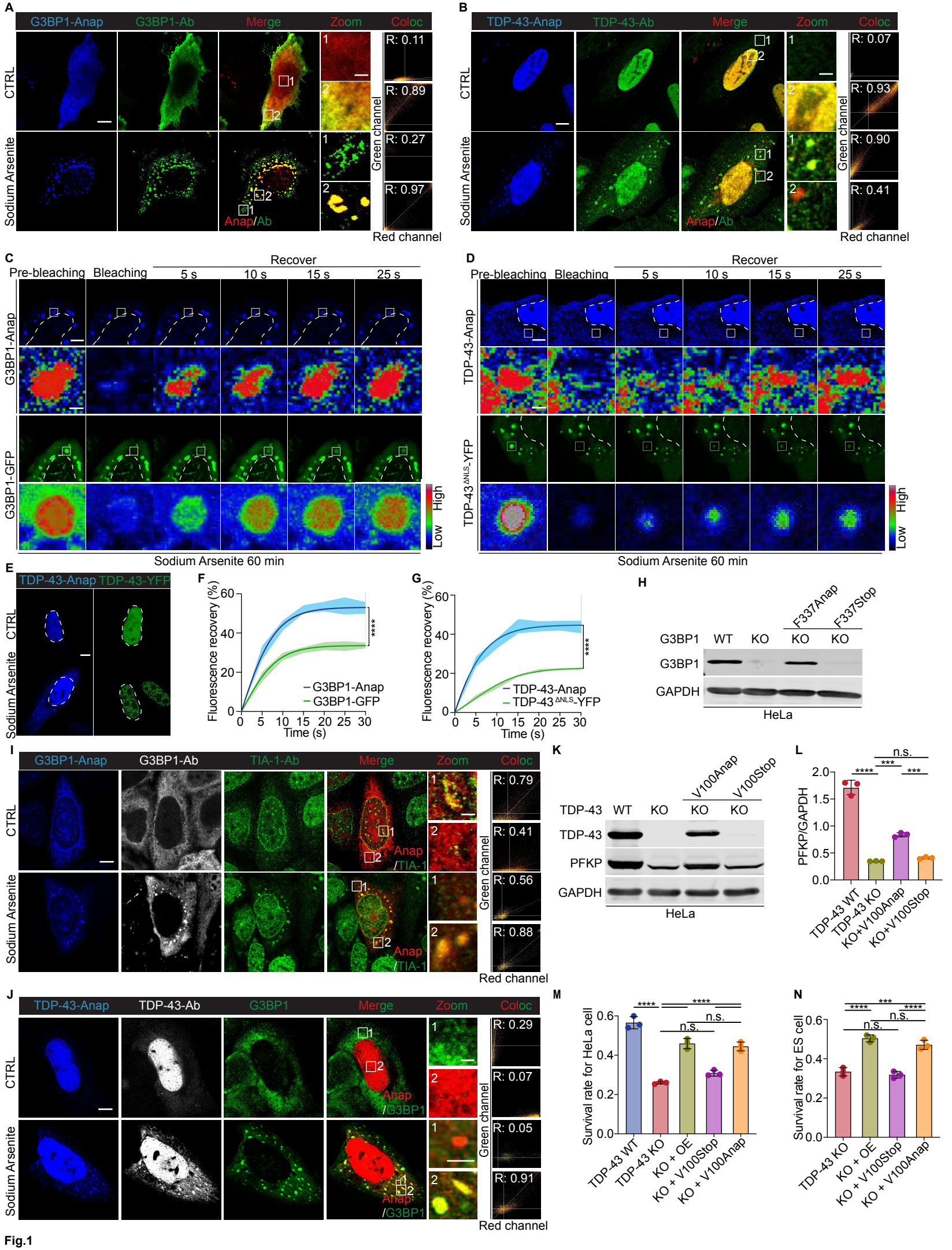
A
G3BP1-Anap
G3BP1-Ab
Merge
Zoom
Coloc
CTRL
Sodium Arsenite
Anap/Ab
R: 0.11
R: 0.89
R: 0.27
R: 0.97
Green channel
Red channel
B
TDP-43-Anap
TDP-43-Ab
Merge
Zoom
Coloc
CTRL
Sodium Arsenite
Anap/Ab
R: 0.07
R: 0.93
R: 0.90
R: 0.41
Green channel
Red channel
C
Pre-bleaching
Bleaching
Recover
5 s
10 s
15 s
25 s
G3BP1-Anap
G3BP1-GFP
High
Low
Sodium Arsenite 60 min
D
Pre-bleaching
Bleaching
Recover
5 s
10 s
15 s
25 s
TDP-43-Anap
TDP-43ΔNLS-YFP
High
Low
Sodium Arsenite 60 min
E
TDP-43-Anap
TDP-43-YFP
CTRL
Sodium Arsenite
F
Fluorescence recovery (%)
Time (s)
G3BP1-Anap
G3BP1-GFP
****
G
Fluorescence recovery (%)
Time (s)
TDP-43-Anap
TDP-43ΔNLS-YFP
****
H
F337Anap
F337Stop
G3BP1
WT
KO
KO
KO
G3BP1
GAPDH
HeLa
I
G3BP1-Anap
G3BP1-Ab
TIA-1-Ab
Merge
Zoom
Coloc
CTRL
Sodium Arsenite
Anap /TIA-1
R: 0.79
R: 0.41
R: 0.56
R: 0.88
Green channel
Red channel
K
V100Anap
V100Stop
TDP-43
WT
KO
KO
KO
TDP-43
PFKP
GAPDH
HeLa
L
PFKP/GAPDH
n.s.
****
***
***
TDP-43 WT
TDP-43 KO
KO+V100Anap
KO+V100Stop
J
TDP-43-Anap
TDP-43-Ab
G3BP1
Merge
Zoom
Coloc
CTRL
Sodium Arsenite
Anap /G3BP1
R: 0.29
R: 0.07
R: 0.05
R: 0.91
Green channel
Red channel
M
Survival rate for HeLa cell
****
****
n.s.
n.s.
TDP-43 WT
TDP-43 KO
KO + OE
KO + V100Stop
KO + V100Anap
N
Survival rate for ES cell
***
****
****
n.s.
n.s.
TDP-43 KO
KO + OE
KO + V100Stop
KO + V100Anap

Fig.1

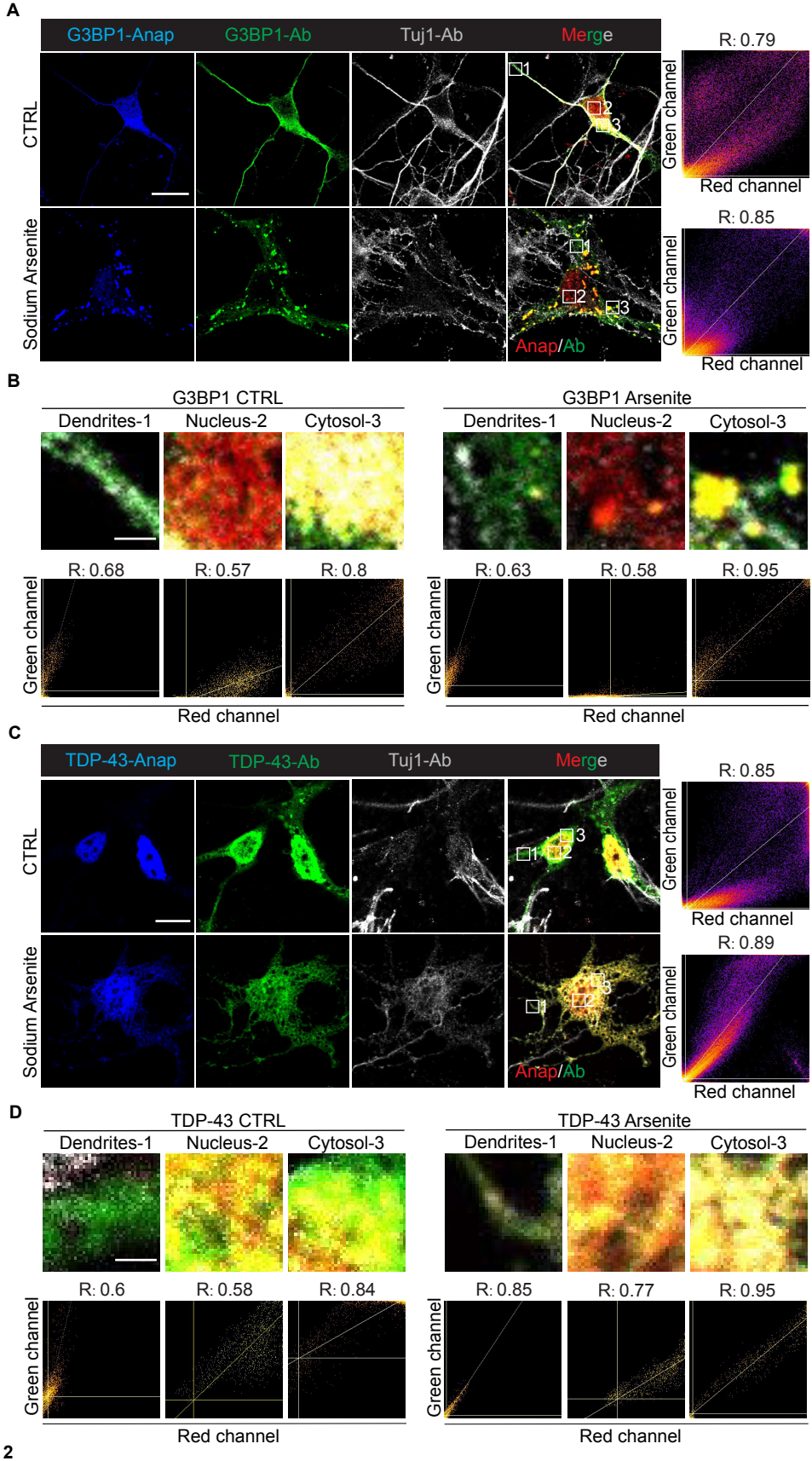
A
G3BP1-Anap
G3BP1-Ab
Tuj1-Ab
Merge
CTRL
Sodium Arsenite
R: 0.79
R: 0.85
Green channel
Red channel
Anap/Ab
B
G3BP1 CTRL
G3BP1 Arsenite
Dendrites-1
Nucleus-2
Cytosol-3
R: 0.68
R: 0.57
R: 0.8
R: 0.63
R: 0.58
R: 0.95
C
TDP-43-Anap
TDP-43-Ab
R: 0.85
R: 0.89
D
TDP-43 CTRL
TDP-43 Arsenite
R: 0.6
R: 0.58
R: 0.84
R: 0.85
R: 0.77
R: 0.95

Fig. 2

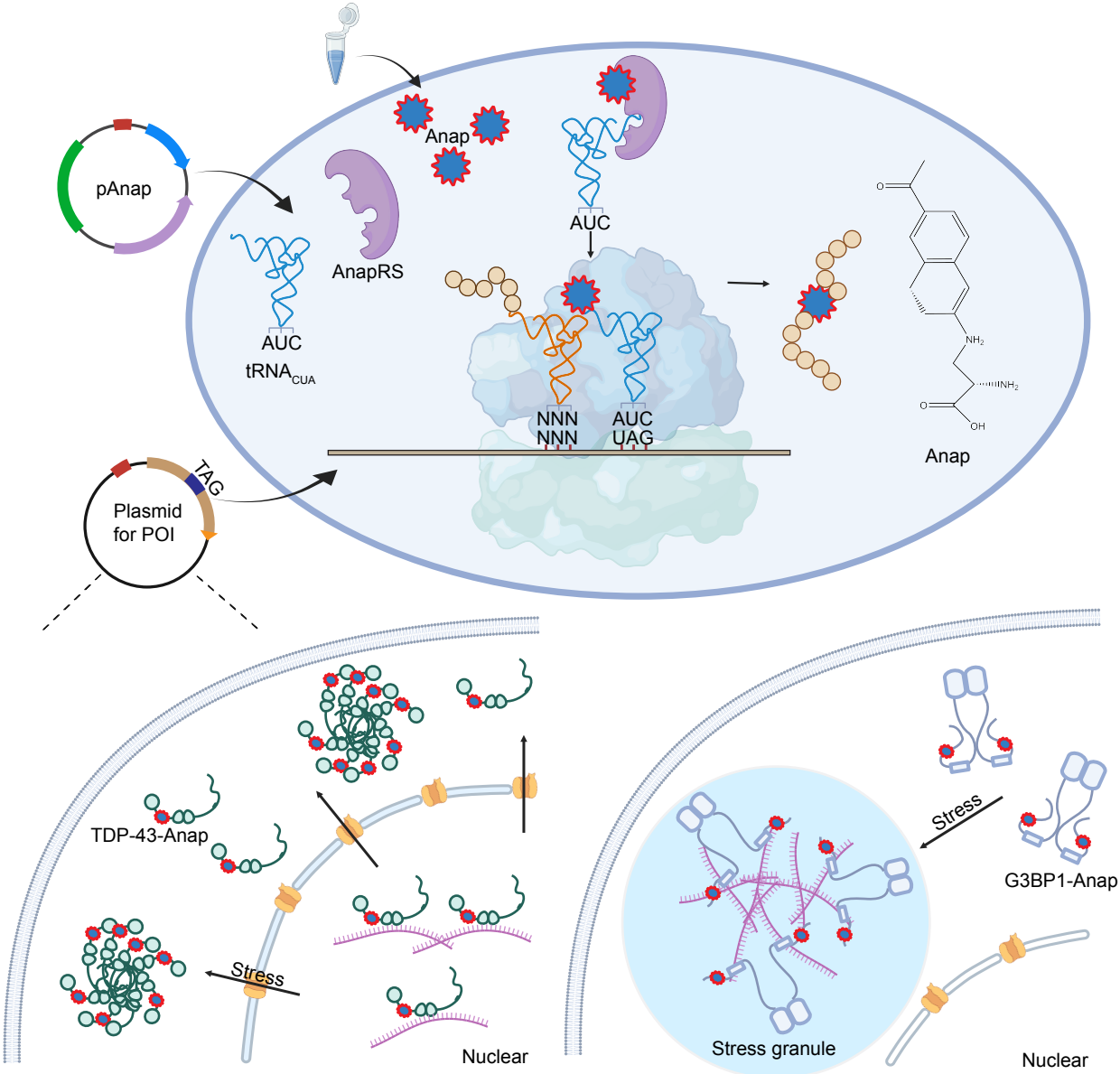
pAnap
Anap
AnapRS
AUC
tRNA$_{CUA}$
AUC
NNN
NNN
AUC
UAG
Anap
Plasmid
for POI
TAG
TDP-43-Anap
Stress
Nuclear
Stress
G3BP1-Anap
Stress granule
Nuclear

Fig. 3